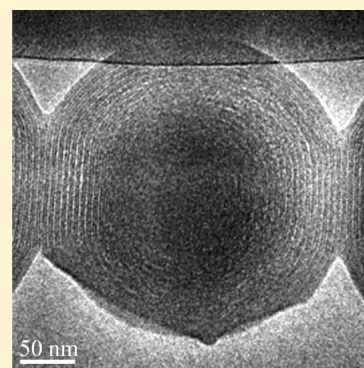


Effect of Polyelectrolyte Stiffness and Solution pH on the Nanostructure of Complexes Formed by Cationic Amphiphiles and Negatively Charged Polyelectrolytes

Maor Ram-On, Yachin Cohen, and Yeshayahu Talmon*

Department of Chemical Engineering and The Russell Berrie Nanotechnology Institute (RBNI), Technion – Israel Institute of Technology, Haifa 3200003, Israel

ABSTRACT: The interaction between amphiphiles and polyelectrolytes has been widely investigated in recent years due to their potential application in industry and medicine, with special focus on gene therapy. The cationic lipid dioleoyl trimethylammonium propane, DOTAP, and the oppositely charged polyelectrolytes, sodium poly(acrylic acid) and sodium poly(styrenesulfonate), form multilamellar complexes in water. Because of the different molecular stiffness of the two polyelectrolytes, they form different nanostructured complexes. Also, because of the different ionization behavior of the two polyelectrolytes, pH differently affects the complexation of the polyelectrolytes with didodecyldimethylammonium bromide (DDAB), another cationic surfactant. We used cryogenic temperature transmission electron microscopy (cryo-TEM) and small-angle X-ray scattering (SAXS) to compare the nanostructures formed. Our results show that although the basic nanostructures of the complexes are always lamellar (multilamellar or unilamellar) the morphology of the complexes is affected by the polyelectrolyte rigidity and the solution pH.



INTRODUCTION

The interaction between polyelectrolytes and low-molecular-weight amphiphiles has been extensively investigated due to their importance in many applications. Many industrial formulations, such as water-based paints, detergents, and cosmetic products, contain both water-soluble polymers and surfactants. In biotechnological applications and in biological systems, the interactions between double-tailed amphiphiles, especially lipids, and different macromolecules are most significant.^{1–3} The binding of polyelectrolytes to oppositely charged amphiphiles is dominated by electrostatic interactions, but hydrophobic forces also play an important role.⁴ Li et al.⁵ showed in a recent study that the cooperative binding strength increases in relation to the square of the polyelectrolyte's linear charge density and in proportion to the amphiphile hydrophobicity. Chemical composition, linear charge density, location of the charges, and flexibility of the backbone of the chain are some of the properties affecting the interactions between polyelectrolytes and charged amphiphiles. Previous studies showed by small-angle X-ray scattering (SAXS) that cationic lipids, namely, dioleoyl trimethylammonium propane (DOTAP) and dioleoylphosphatidylcholine (DOPC) as a neutral “helper-lipid”, and DNA form multilamellar complexes, where the DNA is found between adjacent lipid bilayers, or that the DNA is coated by lipid monolayers in a hexagonal lattice.⁶ Later cryogenic temperature transmission electron microscopy (cryo-TEM) work clarified the elaborate mechanism of multilamellar complex formation in several different systems.^{7,8}

Complexation between DOTAP and sodium poly(acrylic acid), NaPAA, was studied by Bordi et al.⁹ They described the

morphology of the polyelectrolyte/lipid complex as clusters of cationic liposomes “glued” together by the polyelectrolyte; however, their characterization technique, staining-and-drying TEM, is an artifact prone methodology.¹⁰ Volodkin et al.¹¹ investigated the interaction of phosphocholine-based liposomes and oppositely charged poly-L-lysine using dynamic light scattering (DLS), electrophoretic mobility, and differential scanning calorimetry (DSC). Golan et al.¹² studied by cryo-TEM, DLS, and ζ -potential measurements the complexes formed between the synthetic lipid bis(*n*-ferrocenylundecyl) dimethylammonium bromide (BFDMA) and sodium poly(acrylic acid) (NaPAA) and between DOTAP and NaPAA at charge ratio (namely, the ratio between overall negative to positive charges in the system), CR, of 1. Rozenfeld et al.¹³ showed that addition of oligonucleotide (ODN) to dioctadecyldimethylammonium bromide (DODAB) solutions induced the formation of multilamellar structures from the unilamellar vesicles. They used SAXS, DSC, and electron spin resonance (ESR). Of course, many other systems based on lipid-like molecules have also been studied, forming complexes with DNA, such as cyclodextrin derivatives, for example, Li et al.¹⁴

Here we report the characterization of the nanostructure of complexes between the cationic lipid DOTAP and two different polyelectrolytes, NaPAA and NaPSS (sodium poly styrenesulfonate).

Special Issue: William M. Gelbart Festschrift

Received: February 2, 2016

Revised: March 24, 2016

Published: April 6, 2016

fonate). The different systems were investigated at different charge ratios between 0.5 and 2. We studied DOTAP systems, as a starting point, due to its importance in transfection. Indeed, multilamellar onion-like structures between DOTAP and DNA have been previously reported in systems containing oligonucleotide or DNA and DOTAP using direct and indirect characterization methods.^{8,15,16}

Another crucial parameter in the system that could influence its nanostructure is the solution pH. Many polyelectrolytes are weak acids or bases, and thus their chemical structure could be affected by solution pH. Thongngam and McClements¹⁷ studied solutions of SDS, an anionic surfactant, and chitosan, a cationic biopolymer. Lam and Walker¹⁸ studied solutions containing cetyltrimethylammonium bromide, C₁₆TAB, a cationic surfactant, and poly(4-vinyl benzoate), PVB, by DLS, SANS (small-angle neutron scattering), NMR (nuclear magnetic resonance), and solubility measurements, to map pH effects on the system.

We have studied the effect of pH on the self-assembly of DDAB, a double-tailed cationic surfactant, which allowed us much more flexibility in the experimental work, with the two polyelectrolytes previously mentioned: NaPAA and NaPSS. We have applied cryo-TEM for direct comparison between the nanostructures obtained in the systems. Our results suggest that the aggregate morphology depends on the polyelectrolyte properties, particularly its molecular stiffness. Also, pH may have a dominant role in self-assembly of oppositely charged molecules, depending on the polyelectrolyte.

EXPERIMENTAL SECTION

The cationic lipid DOTAP was purchased from Avanti Polar Lipids. The chloroform of the original DOTAP solution was removed by nitrogen gas, and the dried lipid was kept in a vial overnight under vacuum to remove traces of chloroform. Afterward, appropriate volume of water was added to the DOTAP film to obtain 1 mM dispersions. The dispersion was sonicated using a tip-sonicator (Heat Systems-Ultrasonic, New York) at 25 °C for 2 min, until it clarified. We purchased the cationic surfactant DDAB ($\geq 98\%$) from Fluka and used it without further purification. An appropriate amount of DDAB was dissolved in water to obtain final concentration of 5 mg/mL. We sonicated the dispersions by the same tip-sonicator. See Figure 1 for the molecular structures of the compounds used here.

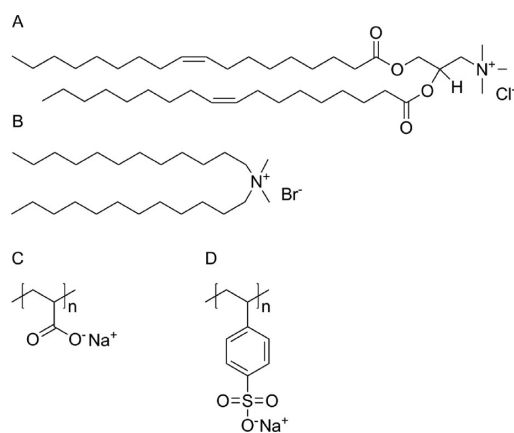


Figure 1. Chemical structure of: (A) DOTAP, (B) DDAB, (C) NaPAA, and (D) NaPSS.

The anionic polyelectrolytes NaPAA (average MW ≈ 15 kDa) and NaPSS (average MW ≈ 70 and 1000 kDa) were purchased from Sigma-Aldrich as 35, 30, and 25 wt % aqueous solutions, respectively. The solutions were diluted between 5 and 500 times, depending on desired final concentration of lipid/polyelectrolyte. NaPAA or NaPSS solutions were added to the 1 mM lipid dispersion in appropriate amounts to produce polyelectrolyte/lipid CR of 0.5, 1, and 2. (The DOTAP final concentration was between 0.77 and 0.97 mM.) CR was estimated as the ratio between the negatively charged groups of the polyelectrolyte and the positively charged headgroups of the lipids.

Proper amounts of polyelectrolyte (NaPAA or NaPSS) solutions were added to the DDAB solutions to obtain a constant charge ratio of 1. Complexes were left overnight to equilibrate at 37 °C. That temperature was chosen to ensure samples were prepared well above the surfactant gel-to-liquid transition point ($T_m \approx 16$ °C in water).¹⁹ The dispersion pH was measured, and HCl or NaOH were added to modify pH to requested values. To compare the system of DDAB and NaPAA to the system of DDAB and NaPSS, we used NaPSS with molecular weight of the same order of magnitude (70 kDa; the molecular weight of NaPAA was 15 kDa).

Cryo-TEM specimens were prepared in a controlled environment vitrification system (CEVS) at 25 °C for DOTAP-containing solutions and at 37 °C for DDAB-containing solutions, always at 100% relative humidity, to prevent evaporation from the specimen, as described elsewhere.^{20,21} Prior to specimen preparation, the grids were plasma-etched in a PELCO EasiGlow glow-discharger (Ted Pella, Redding, CA) to increase their hydrophilicity. We imaged the specimens by an FEI Tecnai T12 G² transmission electron microscope, equipped with LaB₆ electron gun, operating at 120 kV. Specimens were equilibrated in the microscope below -178 °C in a Gatan 626 or an Oxford CT-3500 cryo-holders and imaged using a low-dose imaging procedure to minimize electron-beam radiation damage.²² Images were recorded digitally by a Gatan US1000 CCD camera using the DigitalMicrograph software package.

SAXS experiments were performed using a small-angle diffractometer, Molecular Metrology SAXS system with Cu K α radiation from a sealed microfocus tube (MicroMax-002+S), two Göbel mirrors, and three pinholes. The generator was powered at 45 kV and 0.9 mA. The scattering patterns were recorded by a 20 \times 20 cm 2D position-sensitive wire detector with 200 μ m resolution that was positioned 150 cm behind the sample. Acquisition times ranged from about 5 to 48 h for the concentrated to dilute systems, respectively. The solutions were sealed in thin-walled glass capillaries, ~ 2 mm in diameter and 0.01 mm wall thickness, and measured under vacuum at 25 °C for DOTAP and at 37 °C for DDAB. The concentrated gel of DDAB/NaPAA and DDAB/NaPSS was obtained using centrifugation of the complex dispersion for 1 h at 1280g, using a CN-2060 LED & Multifunction type centrifuge (MRC, Israel). The examined gel was sealed in a flat mica-covered cuvette (1.3 mm thick, Linkam)

The scattered intensity $I(q)$ was recorded in the interval $0.07 < q < 2.7$ nm⁻¹, where q is the scattering vector, defined as $q = (4\pi/\lambda) \sin(\theta)$, where 2θ is the scattering angle and λ is the radiation wavelength (0.1542 nm). $I(q)$ was normalized to time, solid angle, primary beam intensity, capillary diameter, transmission, and the Thompson factor.²¹ Scattering of the

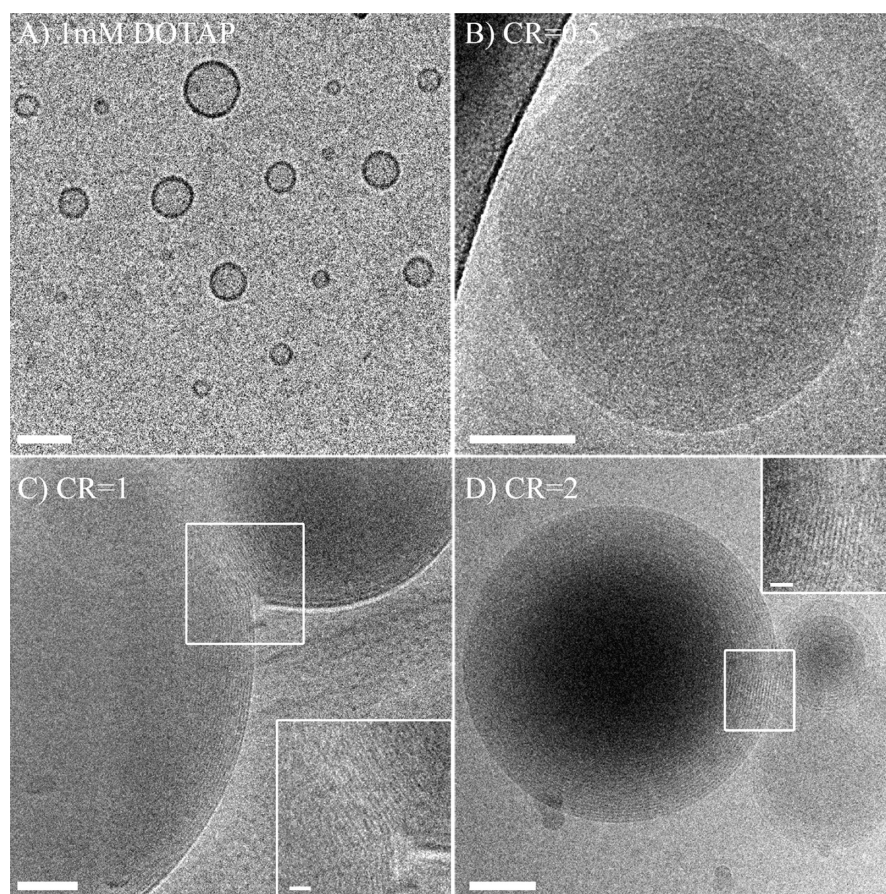


Figure 2. Cryo-TEM images of DOTAP and NaPAA solutions. DOTAP/NaPAA final concentrations are 1/0, 0.95/0.003, 0.9/0.006, and 0.82/0.010 mM, at increasing charge ratio. Insets show higher magnifications of the white rectangles. Bars correspond to 50 nm in the main pictures and to 10 nm in the insets.

empty capillary and electronic noise was subtracted. Solvent scattering was not subtracted.

RESULTS AND DISCUSSION

Effect of Chain Stiffness and Molecular Weight.

Double-tailed lipids such as DOTAP are known to form liposomes in aqueous media. The main aggregates formed upon dispersion of DOTAP in water followed by sonication are unilamellar vesicles, whose size depends on the method of preparation. When a double-tailed lipid is complexed with a negatively charged polyelectrolyte, multilamellar liposomes are the most favorable aggregates, where layers of the lipid confine the polyelectrolyte between them. This structure was already seen in the system of DOTAP and DNA at $CR = 1$.^{6,23} Here we have investigated the complexation of DOTAP with polyelectrolytes other than DNA to show the generality of the phenomenon and to study the effect of a number of parameters, as previously described. PAA and PSS are both negatively charged polyelectrolytes, but they differ in rigidity; whereas PAA is a very flexible polymer, with persistence length of 1 nm,²⁴ PSS is much stiffer due to sulfate groups limiting the polyelectrolyte conformation, with a persistence length of 10 nm.^{24,25} Because complexation between a cationic lipid or a surfactant and an oppositely charged polyelectrolyte is mainly electrostatically driven,²⁶ we examined the systems at different charge ratios, between 0.5 and 2, while maintaining the lipid concentration almost constant. In addition, we checked the

complexation of DOTAP of two different molecular weight NaPSS (70 and 1000 kDa) to assess the effect of chain length.

We first examined the self-aggregation of the lipid alone in aqueous solution. As expected, large unilamellar vesicles are obtained (Figure 2A). The addition of the polyelectrolyte to DOTAP at $CR = 1$ led to the formation of multilamellar complexes, where the polyelectrolyte is most probably sandwiched between adjacent layers. This phenomenon had been reported in the literature for complexation of cationic lipids with DNA^{23,27,28} or oligonucleotides.⁸ The multilamellar complexes varied in size and in number of layers. We lowered and raised CR below and above unity and followed the morphological changes in the DOTAP–NaPAA and DOTAP–NaPSS systems.

Addition of NaPAA. NaPAA (15 kDa) was added to charge ratios of 0.5, 1, and 2, which resulted in lipid concentration of 0.95, 0.90, and 0.82 mM. That led to the formation of round multilamellar complexes with tight but distinguishable layers (Figure 2B–D). The complex size is polydispersed, from hundreds of nanometers to about 1 μm . We expected the effect of the charge ratio to be stronger; that is, we expected the clusters of aggregates to form only in charge ratio around 1 because at that point the aggregates are neutral and are not repelled from each other. When the charge ratio is below or above 1, the aggregates are either positive or negative, leading to repulsion forces between them; however, clusters were also seen at charge ratio of 2 (Figure 2D). This could be explained by local charge caused by uneven coverage of polyelectrolyte

molecules of the surface of the complex, leaving exposed free lipid head groups that could be attracted to polyelectrolyte molecules located on a nearby complex, resulting in polyelectrolyte bridging. According to the SAXS measurement, the CR does not have a significant effect on the periodic spacing of ~ 4.7 nm (Table 1). Furthermore, it can be deduced

Table 1. SAXS Measurements of Interlamellar Distances in DOTAP–Polyelectrolyte Systems^a

formulation	CR	d (nm)
DOTAP+NaPAA _{15kD}	0.5	4.71
DOTAP+NaPAA _{15kD}	1	4.65
DOTAP+NaPAA _{15kD}	2	4.73
DOTAP+NaPSS _{70kD}	0.5	4.60
DOTAP+NaPSS _{70kD}	1	4.63
DOTAP+NaPSS _{70kD}	2	4.58
DOTAP+NaPSS _{1000kD}	0.5	4.65
DOTAP+NaPSS _{1000kD}	1	4.63
DOTAP+NaPSS _{1000kD}	2	4.65

^aEstimated error in d -spacing measurement is ± 0.03 nm for CR = 0.5 and ± 0.02 for the others.

from the SAXS curve in Figure 3 that CR has an effect on the complexation and that the extent of complexation is optimal when the polyelectrolyte is in excess. (The peak is higher for larger CR.)

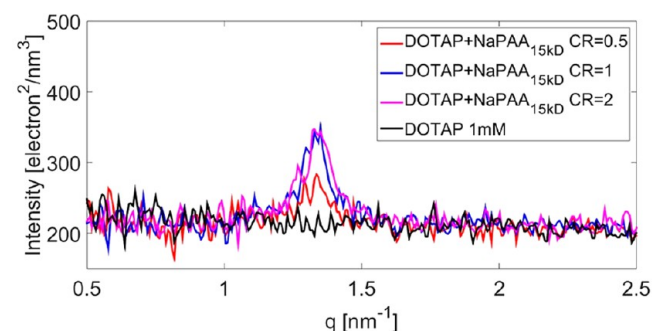


Figure 3. Scattering curves of DOTAP/NaAA complexes at 25 °C. Concentrations are given in Figure 2.

Addition of NaPSS. NaPSS was added to obtain charge ratios of 0.5, 1, and 2, resulting in lipid concentration of 0.93, 0.87, and 0.77 mM for polyelectrolyte with average molecular weight of 70 kDa and 0.92, 0.85, and 0.75 mM for the polyelectrolyte with average molecular weight of 1000 kDa. The addition of NaPSS led to the formation of multilamellar complexes, but the complexes were not round and globular as they were with the NaPAA (Figure 4). Images in the left column show the complexation with 70 kDa NaPSS (Figure 4A–C), and those in the right column show the complexation with 1000 kDa NaPSS (Figure 4D–F). The alternating layers of lipid and polyelectrolyte are clearly resolved, but they form arbitrary aggregates, not well-defined concentric round shapes, similar to complexes formed between cationic lipids and DNA. Moreover, as previously mentioned, NaPAA has a persistence length of ~ 1 nm, while that of NaPSS is ~ 10 nm. This difference in persistence length may influence the capability of the polymer to organize in round nice spherical structures, as can be seen for DOTAP and PAA. For comparison, the persistence length of double-stranded DNA is 50 nm, which

explains the similarity between the NaPSS and DOTAP nanostructures, and DNA and another double-tailed cationic lipid, BFDMA, in the work of Pizzey et al.²⁹ Our SAXS data (Table 1) indicate that the periodic spacing in the multilamellar structure of DOTAP and NaPSS is ~ 4.6 nm, similar to that in the DOTAP/NaPAA system. The molecular weight of the polyelectrolyte does not seem to influence the interlamellar spacing of the complexes in the range studied. Here, too, it can be seen from the scattering plots (Figure 5) that optimal complexation, as determined by peak height, is observed when the polyelectrolyte is in excess.

Effect of pH. In this part of our work we used DDAB, a double-tailed cationic amphiphile, which forms large vesicles when dispersed in water. Although it has some similarities to DOTAP, its tails are shorter (12 carbon atoms instead of 18), it has a simpler chemical structure, and is more soluble in water than the lipid. Cryo-TEM of 5 mg/mL (10.8 mM) of DDAB aqueous solution showed that vesicle diameter was between tens of nanometers to about a micrometer (Figure 6). The preparation of cationic vesicles of this surfactant in aqueous solution should take into account its gel-to-liquid phase transition temperature (T_m). Below this temperature the surfactants are poorly soluble in water. Samples were kept and prepared at 37 °C, well above T_m of 16 °C. As expected, the addition of polyelectrolytes induced the formation of multilamellar complexes, in which the polyelectrolyte molecules are sandwiched between adjacent surfactant layers, screening the electrostatic repulsion; however, altering pH using HCl and NaOH emphasized the inherent difference between the two examined polyelectrolytes, as clearly demonstrated here by cryo-TEM.

NaPAA and NaPSS were added to the charge ratio of 1, which resulted in surfactant final concentration of 4.47 mg/mL (9.66 mM) and 4.84 mg/mL (10.47 mM). Using HCl and NaOH, we lowered the pH to 2.4 to 2.5, well below NaPAA pK_a value, or increased it to 11.4 to 11.5.

Addition of NaPAA. The pH upon mixing of DDAB and NaPAA at CR = 1 was measured as 7.4. As shown in Figure 7B, cryo-TEM images show multilamellar complexes. These multilamellar complexes are made of alternating layers of the surfactant and the polyelectrolyte. It also can be seen that the complexes tend to aggregate at this pH and CR. Raising the pH to 11.4 with NaOH did not seem to have any effect on the nanostructure (Figure 7C). In contrast, lowering the pH to 2.4 promoted massive change in morphology, namely, the formation of unilamellar vesicles (Figure 7A). This can be explained by the polyelectrolyte nature, which is pH-sensitive. At high pH values, higher than pK_a (~ 4.2), most of the polyelectrolyte carboxyl groups are deprotonated and carry a negative charge. The surfactant is positively charged, so the electrostatic attraction is strong, leading to the formation of multilamellar aggregates. As pH is lowered the carboxylic groups on the NaPAA backbone remain neutral, and the attraction between the surfactant and polyelectrolyte molecules weakens. At low enough pH, a critical value of uncharged groups (protonated groups) is exceeded, and it is no longer energetically favorable to form multilamellar complexes; the surfactant molecules prefer to maintain their unilamellar vesicle structure without additional layers. SAXS measurements strengthen this assumption, as can be seen from Figure 8. As pH is lowered the peak becomes smaller until it is negligible at pH 2.8, similar to pure DDAB solution. Also, the results demonstrate a mild change (0.5 Å) of the interlamellar spacing

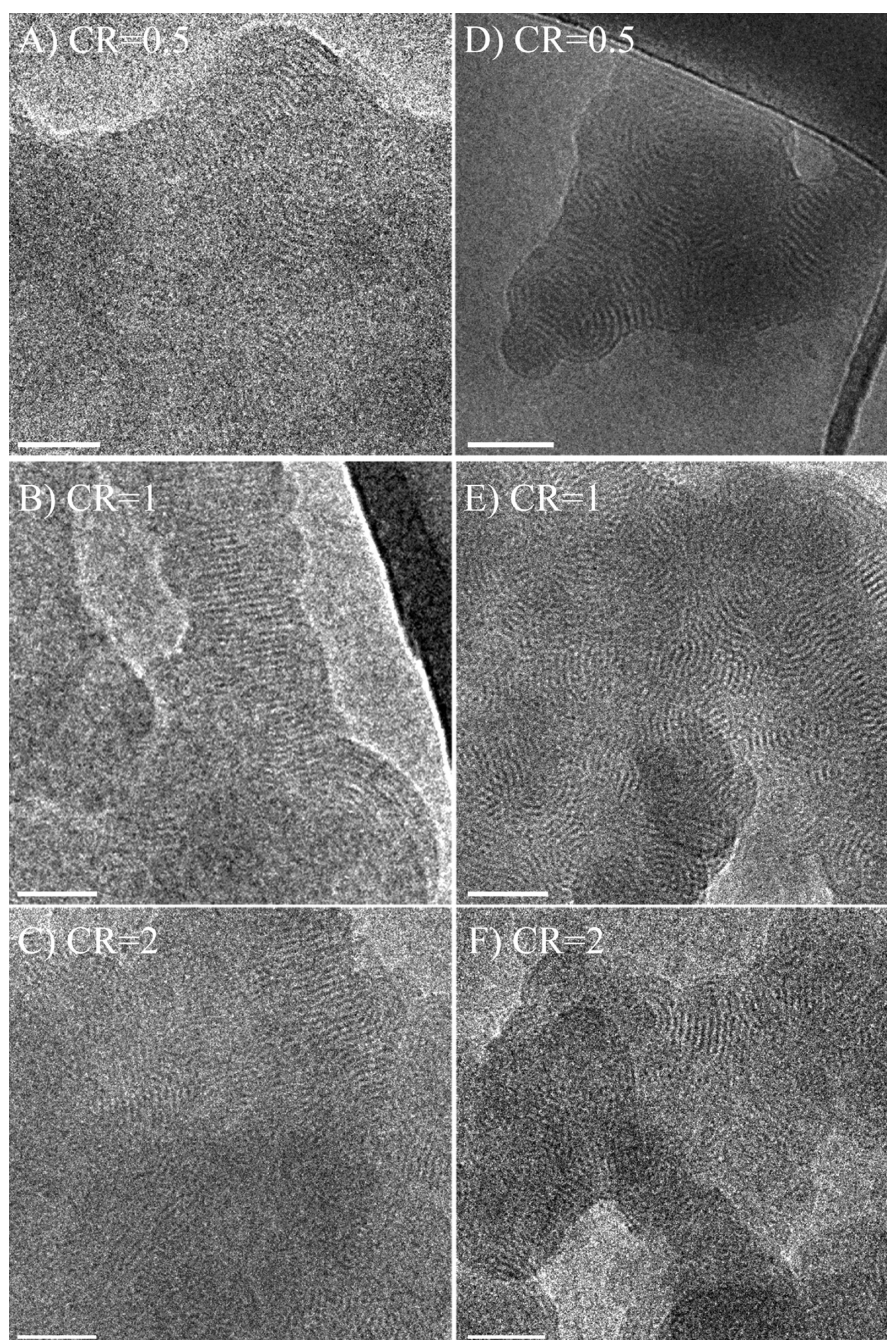


Figure 4. Cryo-TEM images of DOTAP and NaPSS: MW \approx 70 kDa, DOTAP/NaPSS concentrations are 0.93/0.0014, 0.87/0.0026, 0.77/0.045 mM, as charge ratio increases (left column); MW \approx 1000 kDa, DOTAP/NaPSS concentrations are 0.92/0.0001, 0.85/0.0002, 0.74/0.0003 mM, as charge ratio increases (right column). Bars correspond to 50 nm.

as pH is altered (from 3.36 to 3.31 nm), as can be seen in Table 2. This change may stem from electrostatic attraction that increases as pH is raised, leading to a tighter packing and consequently to a smaller spacing. Li et al.⁵ showed that stiffer polyelectrolytes showed weaker binding to the surfactant molecules compared with a more flexible polyelectrolyte. It can be seen from Table 2 that the spacing is indeed smaller for the more flexible polymer (NaPAA), indicating stronger binding and attraction. These results are in agreement with the results of Vivares and Ramos,³⁰ who studied complexation of DDAB with an alternating copolymer of styrene and maleic acid in its sodium salt form as the negatively charged polyelectrolyte. They found a periodic distance to be \sim 3 nm.

The similarities between that copolymer and PAA suggest that both polymers are themselves somewhat amphiphilic, so that while their charged groups tend to interact with the oppositely charged surfactant heads, their hydrophobic segments interact with the hydrophobic part of the surfactant at the water interface.

Addition of NaPSS. The pH upon mixing of DDAB and NaPSS at CR = 1 was measured as 4.7. Cryo-TEM showed multilamellar structures in this system (Figure 7E); however, pH variation to higher (11.5) and lower (2.5) values did not affect the observed nanostructure. Here, too, the explanation stems from the PSS properties. The polystyrenesulfonate side group acts as a strong acid, and the protons are dissociated at

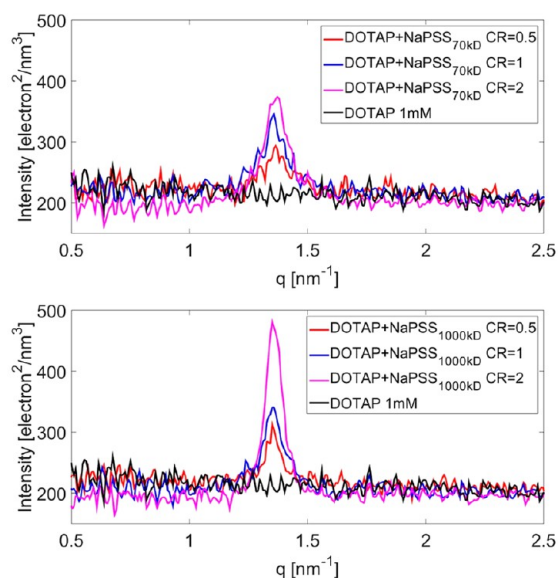


Figure 5. SAXS curves of DOTAP/NaPSS complexes at 25 °C. Concentrations are given in Figure 4.

the entire pH range. This leads to charged side groups that preserve electrostatic attraction at all examined pH values. In Figure 7D–F, we image multilamellar aggregates, where the polyelectrolyte is located between adjacent layers of surfactant. SAXS results supported the observation of multilamellar complexes in DDAB/NaPSS systems in the entire pH range tested, as can be seen in Figure 9. The scattering curves demonstrated two peaks, the second being at exactly twice the q value of the first, indicative of a multilamellar structure. Interestingly the first peak is much weaker than the second. That had been documented in systems containing a surfactant with a high electron density near the head groups and particularly reported by Nallet et al.,³¹ who examined lamellar phases of AOT (bis 2-ethylhexyl sodium sulfosuccinate) and water. They demonstrated that as the surfactant concentration is changed the first peak diminishes and even disappears. The electron density around the AOT headgroup is relatively high because it contains sulfonate group. In our case, the polyelectrolyte charged sulfonate groups also are strongly attracted to the charged head of DDAB, which can induce the same effect and cause the first peak to be lower than the second

one. To verify the existence of a lower first peak, we performed additional SAXS experiments after the sample was centrifuged, and only the “cream” containing the complex was taken for measurements to maximize the scattering signal (Figure 10). The ratio of the first and second intensity peaks is in accord with the form factor calculated for a “two-square” electron density profile presented for AOT by Nallet et al.,³¹ with the same parameters of component electron densities and head-group dimension and with a longer hydrocarbon tail of 1.2 nm.

The SAXS results demonstrated that the periodic distance in DDAB/NaPSS complexes is ~ 6 nm. This periodic spacing is significantly larger than that in of the DDAB/NaPAA complexes. Because polystyrenesulfonate is much more hydrophilic than poly(acrylic acid), fully deprotonated at all pH, those charged groups that do not interact with the positively charged headgroups of the surfactant interact with the water molecules. PAA, with a more hydrophobic backbone, adsorbs more tightly to the surfactant lamellar surface, where it may adopt a flatter conformation, while the more hydrophilic PSS chains interact better with water and thus may adopt a more coiled conformation, which leads to a thicker layer and hence a larger periodic distance.

CONCLUSIONS

Cryo-TEM shows that the complexes formed between DOTAP and NaPAA or NaPSS are multilamellar at charge ratios of 0.5 to 2. These nanostructures resemble the self-assembly of cationic lipids with DNA or oligodeoxynucleotide (ODN) into lipoplexes.^{16,28,29} Although all nanostructures are multilamellar, there are morphological differences between them, as imaged by cryo-TEM. These data once again refute the model that assumes polyelectrolyte molecules decorating intact vesicles following complexation. It has been implied that the self-assembly of the oppositely charged molecules is mainly dictated by the nature of the lipid packing,¹² but here we demonstrate that the characteristics of the polymer chain, in particular, flexibility and the state of ionization, are also significant. The difference of one order of magnitude in the persistence length (1 nm compared with 10 nm) between the two polyelectrolytes leads to different morphology of the complexes; however, the molecular weight of same polyelectrolyte does not appear to affect the structure of the complexes.

Using cryo-TEM we also imaged the morphological changes upon pH variation in systems containing a polyelectrolyte that

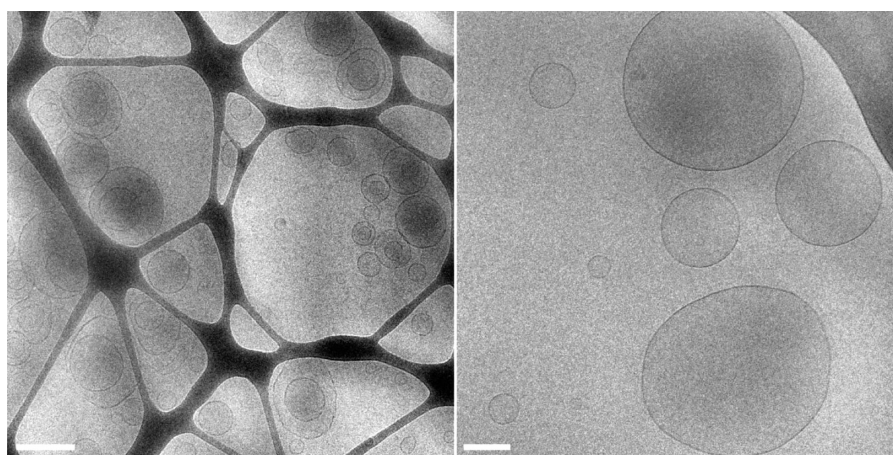


Figure 6. Cryo-TEM images of 5 mg/mL DDAB at 37 °C. Bars correspond to 500 (left) and 100 nm (right).

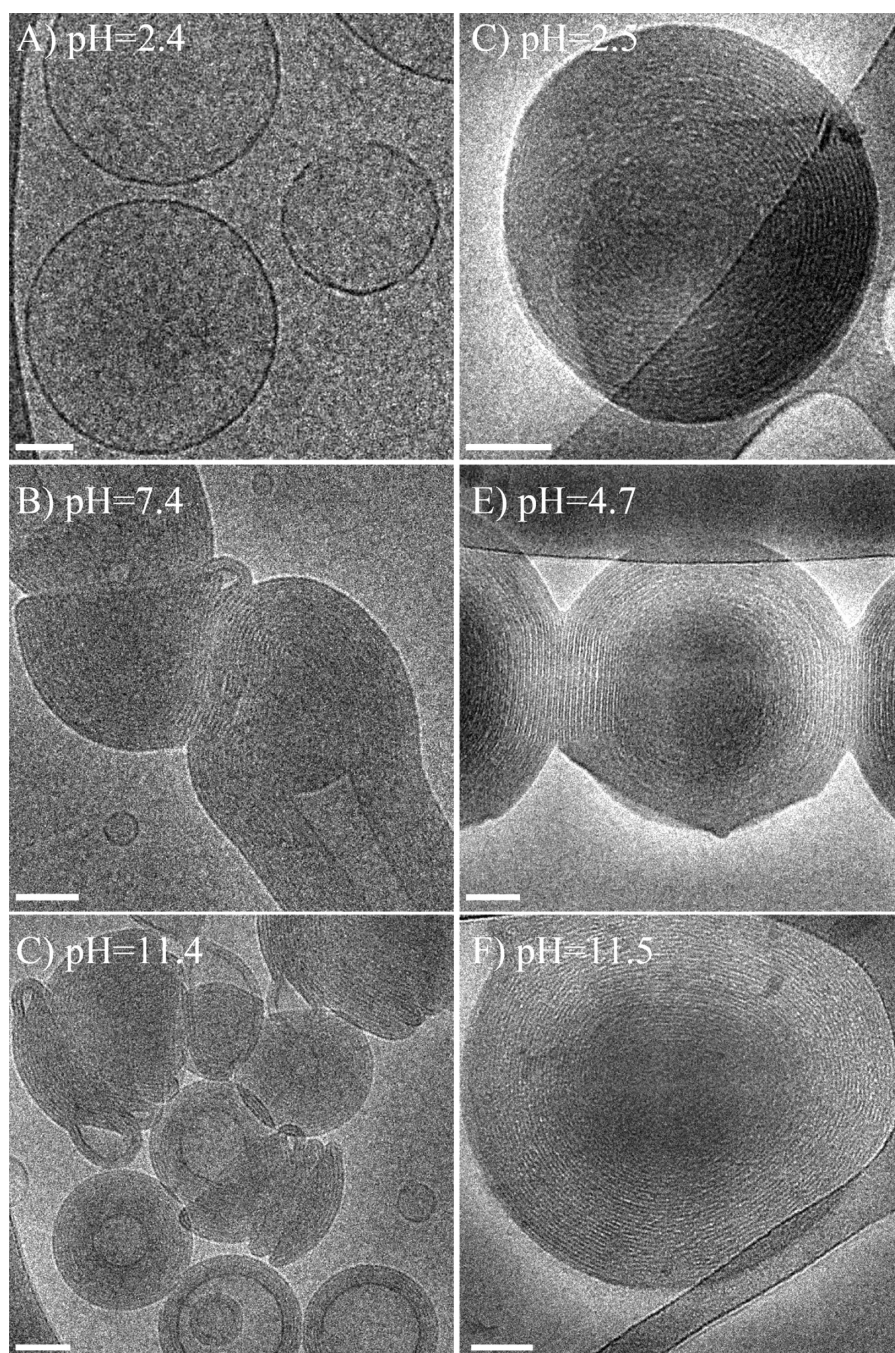


Figure 7. Cryo-TEM images of DDAB and NaPAA (A–C); concentrations are 4.47–0.92 mg/mL. Cryo-TEM images of DDAB and NaPSS (D–F); concentrations are 4.84–2.14 mg/mL. CR = 1 in all. Bars correspond to 50 nm.

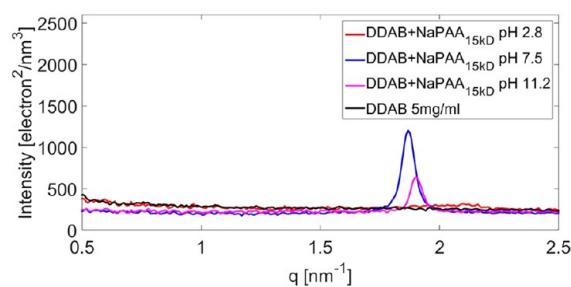


Figure 8. Scattering curves of DDAB/NaPAA complexes at 37 °C. Concentrations are as given in Figure 7.

Table 2. SAXS Measurements of Interlamellar Distances in DDAB–polyelectrolyte Systems with CR of 1^a

formulation	pH	<i>d</i> spacing (nm)
DDAB	8.1	
DDAB+NaPAA	2.8	
DDAB+NaPAA	7.5	3.36
DDAB+NaPAA	11.2	3.31
DDAB+NaPSS	2.5	6.00
DDAB+NaPSS	4.3	6.00
DDAB+NaPSS	11.4	5.99

^aEstimated error in *d*-spacing measurement is ±0.01 nm.

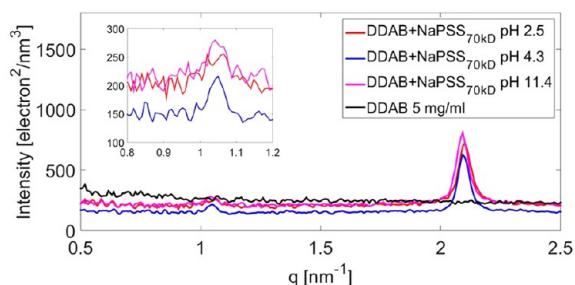


Figure 9. Scattering curves of DDAB/NaPSS complexes at 37 °C. The first peak is magnified in the inset. Concentrations are as given in Figure 7.

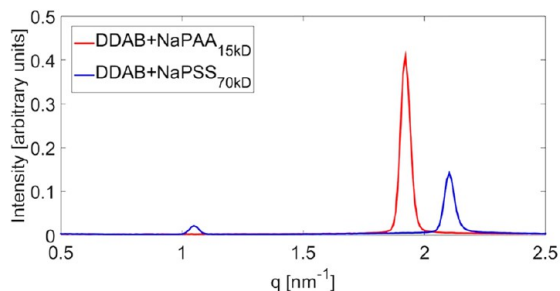


Figure 10. Scattering curves of concentrated DDAB/NaPAA and DDAB/NaPSS complexes at 37 °C.

is a weak acid. Lowering the pH below the pK_a of NaPAA leads to observable change in nanostructure, namely, the transition from multilamellar complexes (at high pH) to unilamellar vesicles, probably of surfactant molecules only, at low pH, because below a critical pH there are insufficient negative charges to energetically favor organization into multilamellar complexes.

SAXS was applied to obtain quantitative information regarding periodic distances of the different complexes. The data obtained were in good agreement with the microscopy and suggested a clear difference between complexes of DDAB/NaPAA and DDAB/NaPSS, where the latter had twice the periodic distance of the other. That is most probably due to the differences in the polyelectrolyte conformation at the surfactant–water interface, with NaPAA being adsorbed more tightly packed, while NaPSS was more coiled. These differences were not observed in the DOTAP/NaPAA and DOTAP/NaPSS systems. It seems that in this case the “lipid” is the dominant factor in the interaction and packing into double layers due to its very hydrophobic tails (18 carbon atoms with one double bond per chain) and the very bulky headgroup. These have apparently much stronger effect on the aggregation than the difference in persistence length of the polyelectrolytes.

AUTHOR INFORMATION

Corresponding Author

*E-mail: ishi@tx.technion.ac.il. Tel: 972-4-8292007.

Notes

The authors declare no competing financial interest.

ACKNOWLEDGMENTS

This work has been partially supported by an Israel Science Foundation (ISF) grant. The cryo-TEM work was performed at the Technion Laboratory for Electron Microscopy of Soft Matter, an infrastructure laboratory of the Technion Russell

Berrie Nanotechnology Institute (RBNI). We thank Dr. Rafail Khalfin of the Technion Department of Chemical Engineering for his assistance with the SAXS measurements.

REFERENCES

- (1) Antunes, F. E.; Marques, E. F.; Miguel, M. G.; Lindman, B. Polymer-Vesicle Association. *Adv. Colloid Interface Sci.* **2009**, *147*–148, 18–35.
- (2) Margolin, A. L.; Sherstyuk, S. F.; Izumrudov, V. A.; Zezin, A. B.; Kabanov, V. A. Enzymes in Polyelectrolyte Complexes. The Effect of Phase Transition on Thermal Stability. *Eur. J. Biochem.* **1985**, *146*, 625–632.
- (3) Shaner, S. L.; Melancon, P.; Lee, K. S.; Burgess, R. R.; Record, M. T., Jr Ion Effects on the Aggregation and DNA-Binding Reactions of Escherichia Coli RNA Polymerase. *Cold Spring Harbor Symp. Quant. Biol.* **1983**, *47* (Pt 1), 463–472.
- (4) Langevin, D. Complexation of Oppositely Charged Polyelectrolytes and Surfactants in Aqueous Solutions. A Review. *Adv. Colloid Interface Sci.* **2009**, *147*, 170–177.
- (5) Li, D.; Wagner, N. J. Universal Binding Behavior for Ionic Alkyl Surfactants with Oppositely Charged Polyelectrolytes. *J. Am. Chem. Soc.* **2013**, *135*, 17547–17555.
- (6) Safinya, C. R. Structures of lipid–DNA Complexes: Supramolecular Assembly and Gene Delivery. *Curr. Opin. Struct. Biol.* **2001**, *11*, 440–448.
- (7) Antunes, F. E.; Brito, R. O.; Marques, E. F.; Lindman, B.; Miguel, M. Mechanisms behind the Faceting of Catanionic Vesicles by Polycations: Chain Crystallization and Segregation. *J. Phys. Chem. B* **2007**, *111*, 116–123.
- (8) Weisman, S.; Hirsch-Lerner, D.; Barenholz, Y.; Talmon, Y. Nanostructure of Cationic Lipid-Oligonucleotide Complexes. *Biophys. J.* **2004**, *87*, 609–614.
- (9) Bordi, F.; Cametti, C.; Diociaiuti, M.; Gaudino, D.; Gili, T.; Sennato, S. Complexation of Anionic Polyelectrolytes with Cationic Liposomes: Evidence of Reentrant Condensation and Lipoplex Formation. *Langmuir* **2004**, *20*, 5214–5222.
- (10) Talmon, Y. Staining and Drying-Induced Artifacts in Electron Microscopy of Surfactant Dispersions. *J. Colloid Interface Sci.* **1983**, *93*, 366–382.
- (11) Volodkin, D.; Ball, V.; Schaaf, P.; Voegel, J.-C.; Mohwald, H. Complexation of Phosphocholine Liposomes with Polylysine. Stabilization by Surface Coverage versus Aggregation. *Biochim. Biophys. Acta, Biomembr.* **2007**, *1768*, 280–290.
- (12) Golan, S.; Talmon, Y. Nanostructure of Complexes between Cationic Lipids and an Oppositely Charged Polyelectrolyte. *Langmuir* **2012**, *28*, 1668–1672.
- (13) Rozenfeld, J. H. K.; Duarte, E. L.; Barbosa, L. R. S.; Lamy, M. T. The Effect of an Oligonucleotide on the Structure of Cationic DODAB Vesicles. *Phys. Chem. Chem. Phys.* **2015**, *17*, 7498–7506.
- (14) Li, Z.; Yin, H.; Zhang, Z.; Liu, K. L.; Li, J. Supramolecular Anchoring of DNA Polyplexes in Cyclodextrin-Based Polypseudorotaxane Hydrogels for Sustained Gene Delivery. *Biomacromolecules* **2012**, *13*, 3162–3172.
- (15) Mel'Nikova, Y. S.; Mel'Nikov, S. M.; Löfroth, J.-E. Physico-Chemical Aspects of the Interaction between DNA and Oppositely Charged Mixed Liposomes. *Biophys. Chem.* **1999**, *81*, 125–141.
- (16) Koltover, I.; Salditt, T.; Safinya, C. R. Phase Diagram, Stability, and Overcharging of Lamellar Cationic lipid–DNA Self-Assembled Complexes. *Biophys. J.* **1999**, *77*, 915–924.
- (17) Thongngam, M.; McClements, D. J. Influence of pH, Ionic Strength, and Temperature on Self-Association and Interactions of Sodium Dodecyl Sulfate in the Absence and Presence of Chitosan. *Langmuir* **2005**, *21*, 79–86.
- (18) Lam, V. D.; Walker, L. M. A pH-Induced Transition of Surfactant-Polyelectrolyte Aggregates from Cylindrical to String-of-Pearls Structure. *Langmuir* **2010**, *26*, 10489–10496.

- (19) Feitosa, E.; Jansson, J.; Lindman, B. The Effect of Chain Length on the Melting Temperature and Size of Dialkyldimethylammonium Bromide Vesicles. *Chem. Phys. Lipids* **2006**, *142*, 128–132.
- (20) Bellare, J. R.; Davis, H. T.; Scriven, L. E.; Talmon, Y. Controlled Environment Vitrification System: An Improved Sample Preparation Technique. *J. Electron Microsc. Tech.* **1988**, *10*, 87–111.
- (21) Talmon, Y. The Study of Nanostructured Liquids by Cryogenic-Temperature Electron Microscopy — A Status Report. *J. Mol. Liq.* **2015**, *210*, 2–8.
- (22) Yan, Y.; Hoffmann, H.; Makarsky, A.; Richter, W.; Talmon, Y. Swelling of L_{α} -Phases by Matching the Refractive Index of the Water-Glycerol Mixed Solvent and that of the Bilayers in the Block Copolymer System of (EO)15-(PDMS)15-(EO)15. *J. Phys. Chem. B* **2007**, *111*, 6374–6382.
- (23) Even-Chen, S.; Cohen, R.; Barenholz, Y. Factors Affecting DNA Binding and Stability of Association to Cationic Liposomes. *Chem. Phys. Lipids* **2012**, *165*, 414–423.
- (24) Walczak, W. J.; Hoagland, D. A.; Hsu, S. L. Analysis of Polyelectrolyte Chain Conformation by Polarized Raman Spectroscopy. *Macromolecules* **1992**, *25*, 7317–7323.
- (25) Krishnaswamy, R.; Mitra, P.; Raghunathan, V. A.; Sood, A. K. Tuning the Structure of Surfactant Complexes with DNA and Other Polyelectrolytes. *Europhys. Lett.* **2003**, *62*, 357–362.
- (26) Kogej, K. Association and Structure Formation in Oppositely Charged Polyelectrolyte–surfactant Mixtures. *Adv. Colloid Interface Sci.* **2010**, *158*, 68–83.
- (27) Safinya, C. R. Structures of Lipid-DNA Complexes: Supramolecular Assembly and Gene Delivery. *Curr. Opin. Struct. Biol.* **2001**, *11*, 440–448.
- (28) Simberg, D.; Weisman, S.; Talmon, Y.; Barenholz, Y. DOTAP (and Other Cationic Lipids): Chemistry, Biophysics, and Transfection. *Crit. Rev. Ther. Drug Carrier Syst.* **2004**, *21*, 257–317.
- (29) Pizzey, C. L.; Jewell, C. M.; Hays, M. E.; Lynn, D. M.; Abbott, N. L.; Kondo, Y.; Golan, S.; Talmon, Y. Characterization of the Nanostructure of Complexes Formed by a Redox-Active Cationic Lipid and DNA. *J. Phys. Chem. B* **2008**, *112*, 5849–5857.
- (30) Vivares, E.; Ramos, L. Polyelectrolyte-Induced Peeling of Charged Multilamellar Vesicles. *Langmuir* **2005**, *21*, 2185–2191.
- (31) Nallet, F.; Laversanne, R.; Roux, D. Modelling X-Ray or Neutron Scattering Spectra of Lyotropic Lamellar Phases: Interplay between Form and Structure Factors. *J. Phys. II* **1993**, *3*, 487–502.